Effect of viscosity on Rayleigh-Taylor and Richtmyer-Meshkov instabilities

Karnig O. Mikaelian
University of California, Lawrence Livermore National Laboratory, Livermore, California 94550
(Received 2 March 1992; revised manuscript received 31 August 1992)

We consider the effect of viscosity on Rayleigh-Taylor (RT) and Richtmyer-Meshkov (RM) instabilities by deriving a moment equation for fluids with arbitrary density and viscosity profiles, including surface tension. We apply our result to the classical case of two semi-infinite fluids with densities ρ_1 and ρ_2 and viscosities μ_1 and μ_2. Treating a shock as an instantaneous acceleration we find that perturbations at the interface undergo damped oscillations when viscosity and surface tension are both present. For pure viscosity the amplitude $\eta(t)$ evolves according to $\eta(t)/\eta(0)=1+(\Delta v A/2k\nu)(1-e^{-2k^2\nu t})$ where Δv is the jump velocity imparted by the shock, $A=(\rho_2-\rho_1)/(\rho_2+\rho_1)$, $\nu=(\mu_1+\mu_2)/(\rho_1+\rho_2)$, $k=2\pi/\lambda$ is the wave number of the perturbation, and t is time. We also consider the turbulent energy in accelerating fluids and calculate the reduction in $E_{\text{turbulent}}$ as a function of ν, and propose experiments to measure the effect of viscosity on RT and RM instabilities.

PACS number(s): 47.20.−k, 52.35.Py, 47.40.Nm

I. INTRODUCTION

The damping effect of viscosity on the Rayleigh-Taylor [1,2] (RT) instability is well known [3,4]: the growth rate γ, instead of increasing indefinitely with k as in the inviscid classical case ($\gamma^2_{\text{classical}}=gkA$), reaches a peak value given approximately by $\gamma^2/gkA=\frac{1}{2}$ and begins to decrease for larger k, approaching zero as $k\to\infty$. In this paper we investigate the effect of viscosity on the Richtmyer-Meshkov [5,6] (RM) instability and, in addition, on the turbulent energy generated by the RT instability. Not surprisingly, we find that both are damped by viscosity.

In a similar vein we have studied [7] the effect of surface tension where the growth rate peaks at $\gamma^2/gkA=\frac{2}{3}$ and begins to decrease for larger k and actually vanishes at a finite wave number k_c. We found that surface tension causes the perturbation amplitude to oscillate in the RM case. As for the turbulent energy generated by the RT instability, we found that it was reduced from classical because surface tension reduces the range as well as the magnitude of the growth rate, i.e., k is limited by $0\le k\le k_c$ and γ is limited by $\gamma^2/gkA\le\frac{2}{3}$ as compared with the classical case where $0\le k\le\infty$ and $\gamma^2/gkA=1$ for all k. Although viscosity by itself does not affect the range, it does reduce the growth rate below classical, particularly at large k, and therefore we expect (and find) reduced turbulent energy.

RT and RM instabilities are important in astrophysics, geophysics, and technological applications such as inertial confinement fusion (ICF) in which we are primarily interested [8]. Physical viscosity plays practically no role in ICF capsules [9], and therefore it cannot act as a stabilizing mechanism. However, there may be other mechanisms, such as ablative stabilization, which act on ICF plasmas to reduce γ below classical [10], and one may mock up such an effect with viscosity in ordinary fluids. Another application is the direct numerical simulation of RT and RM instabilities: many hydrocodes introduce an "artificial viscosity" which, in addition to smoothing out the physical shock, acts to slow down the subsequent flow in two- and three-dimensional simulations [11].

It is substantially more difficult to include the effect of viscosity compared to that of surface tension. To find the exponential growth rate γ in incompressible fluids one must solve the equation

$$D\left[\left[\rho-\frac{\mu}{\gamma}(D^2-k^2)\right]DW-\frac{1}{\gamma}D\mu(D^2+k^2)W\right]+k^2\left[\frac{g}{\gamma^2}D\rho-\frac{k^2}{\gamma^2}\sum_i T_i^{(s)}\delta(y-y_i)\right]W-k^2\left[\rho-\frac{\mu}{\gamma}(D^2-k^2)\right]W+2\frac{k^2}{\gamma}D\mu DW=0\ , \tag{1}$$

subject to appropriate boundary and jump conditions [4]. In this equation $\rho(y)$ denotes density, $\mu(y)$ is the viscosity, $W(y)$ is the perturbed velocity, and D is the operator d/dy, while g denotes a constant acceleration taken to be in the $+y$ direction, k is the transverse wave number $(k_x^2+k_z^2)^{1/2}=2\pi/\lambda$, where λ is the wavelength of the perturbation, and $T_i^{(s)}$ is the surface tension at interface y_i. Without viscosity Eq. (1) reduces to a *second*-order differential equation; with viscosity it is a *fourth*-order differential equation. Because of this added complexity a moment equation approach, which we suggested earlier [12] for the inviscid and tensionless case, becomes even more attractive when viscosity is present. Much of the work in this paper will be based on this approach, rather than solving Eq. (1) directly. Even for the classical density profile which is given by

$$\rho(y)=\rho_1, \quad \mu(y)=\mu_1 \quad \text{for } y<0 \tag{2a}$$

$$\rho(y)=\rho_2, \quad \mu(y)=\mu_2 \quad \text{for } y>0 \tag{2b}$$

the solutions of Eq.(1) are quite complicated (see Refs. [3,4]). After we derive the general moment equation we will apply it to this particular density profile, but note here that a variety of other profiles were considered in our earlier work [12,13] with considerable success.

A brief history will be illuminating. Equation (1) and a variational principle derived from it were first published by Chandrasekhar (surface tension was not considered in his 1955 paper; the inviscid tensionless case goes back to Rayleigh [1].) Equation (1) is quite general and applies to any density profile. Earlier work by Bellman and Pennington [3] was limited to the classical profile. They considered both viscosity and surface tension in the RT instability. In addition to the exact result they wrote down a simplified dispersion relation for the case of pure viscosity:

$$\gamma^2+2k^2\gamma\frac{\mu_2+\mu_1}{\rho_2+\rho_1}-gk\frac{\rho_2-\rho_1}{\rho_2+\rho_1}=0 \; . \tag{3}$$

Apparently unaware of this work Hide [14] applied the variational method of Chandrasekhar to the classical problem, rederived Eq. (3), and found that it compared very favorably with the exact, albeit numerical, results of Chandrasekhar. Soon, however, Reid published a paper [15] pointing out that Hide's derivation was in error—an important term was left out. Since then any reference to Hide's work [14] is invariably accompanied by a reference to Reid's work [15] pointing out Hide's error. Note that the agreement with the exact results was not in question. Indeed, a recent study [16] of Eq. (3) continues to show extremely good agreement (within 11%) with the exact results, so one wonders how Hide obtained a "correct" equation using a "wrong" derivation.

We hope some light will be thrown in the next section where we derive Eq. (3), generalized to include surface tension, using our moment equation approach. In Sec. III we apply it to the RM problem. Concluding remarks make up Sec. IV.

II. RT INSTABILITY

To derive the moment equations we multiply Eq. (1) by W^m and integrate over y. Many terms can be integrated by parts and the resulting "surface terms" set to zero. Our earlier experience [12] indicates that the $m=0$ equation gives the best results and therefore we will consider $m=0$ and 1 only, the latter corresponding to the variational principle mentioned in the Introduction.

For $m=0$ we obtain

$$\gamma^2\int\rho W\,dy+k^2\sum_i T_i^{(s)}W(y_i)+\gamma\int\mu(D^2+k^2)W dy -g\int D\rho W dy=0 \; . \tag{4}$$

For $m=1$ one obtains [17]

$$\gamma^2\int\rho\left[W^2+\frac{1}{k^2}(DW)^2\right]dy+\gamma\int\mu\left[k^2W^2+2(DW)^2+\frac{1}{k^2}(D^2W)^2\right]dy +k^2\sum_i T_i^{(s)}[W(y_i)]^2-g\int D\rho W^2dy=-\gamma\int W^2D^2\mu dy \; . \tag{5}$$

We should note that Eqs. (4) and (5), and indeed all moment equations, are exact and apply to arbitrary density and viscosity profiles. They will produce the exact growth rate γ provided one uses the exact W, and there is the catch. Exact W's can be obtained by solving Eq. (1), but to do so one must know γ. This apparently circular argument merely reflects the fact that Eq. (1) is in the form of a fourth-order eigenvalue equation where W is an eigenfunction associated with an eigenvalue γ. As we have stressed in previous applications of the moment equations they are useful not for obtaining exact γ's but for obtaining explicit, analytic, albeit approximate γ's by using an approximate W. This is in fact the way Hide used Eq. (5).

The approximate W is

$$W_{\text{classical}}=e^{-k|y|} \; , \tag{6}$$

which is the solution to the *inviscid* classical profile, i.e., Eq. (2) with $\mu_1=\mu_2=0$. The presence of surface tension does not affect Eq. (6).

Let us find γ first by using the $m=0$ equation, Eq. (4). Substituting the profile of Eq. (2) and $W_{\text{classical}}$ of Eq. (6) into Eq. (4) the integrations are easily carried out and we get

$$\gamma^2+2k^2\nu\gamma+\frac{k^3T^{(s)}}{\rho_2+\rho_1}-gkA=0 \; , \tag{7}$$

where

$$\nu\equiv(\mu_2+\mu_1)/(\rho_2+\rho_1) \tag{8a}$$

and

$$A\equiv(\rho_2-\rho_1)/(\rho_2+\rho_1) \; . \tag{8b}$$

It is clear that Eq. (7), after setting $T^{(s)}=0$, is in complete agreement with Eq. (3).

We now apply the same procedure to the $m=1$ equation, i.e., substitute Eqs. (2) and (6) into Eq. (5). Several terms in Eq. (5) can be collected together noting that $W_{\text{classical}}$ satisfies $DW=\pm kW$. The result is

$$\gamma^2+2k^2\nu\gamma+\frac{k^3T^{(s)}}{\rho_2+\rho_1}-gkA=-\frac{\gamma k}{\rho_2+\rho_1}\int W^2D^2\mu dy \ . \tag{9}$$

We have deliberately isolated the right-hand side of Eq. (9) because this is the term neglected by Hide for this problem, as criticized by Reid. Hide's result, $\gamma^2+2k^2\nu\gamma-gkA=0$ (he did not include surface tension), follows immediately upon setting the right-hand side of Eq. (9) equal to zero. This is, however, not justified. Integrating it by parts twice the right-hand side becomes $-2k^2\nu\gamma$ which combines with a similar term on the left-hand side to give $4k^2\nu\gamma$. Clearly, this is wrong because it overestimates the effect of viscosity by a factor of 2 and consequently underestimates γ.

Alternatively, one may integrate the right-hand side of Eq. (9) by parts only once (Reid's criticism [15] appears in this form):

$$\begin{aligned}\int W^2D^2\mu\, dy &= -2\int (D\mu)WDW\, dy \\ &= -2(\mu_2-\mu_1)\int \delta(y)WDW\, dy \\ &= -2(\mu_2-\mu_1)W(0)DW(0)\ .\end{aligned} \tag{10}$$

This quantity again does not vanish unless one takes $DW(0)=0$ (or $\mu_1=\mu_2$). The difficulty is associated with the discontinuity of $DW_{\text{classical}}$ at $y=0$, where $DW_{\text{classical}}(0_\pm)=\mp k$. This is a reflection of the fact that $W_{\text{classical}}$ is not an exact eigenfunction for the classical viscous profile since W_{exact}, in addition to being continuous, would have to have a continuous first derivative [4].

The $m=0$ equation, Eq. (4), does not suffer from such ambiguities. It is the generalization of the inviscid tensionless case given earlier [Eq. (5) of Ref. [12]). Since we found it to give better results when applied to density gradient stabilization [12,13], we naturally propose Eq. (4) as the preferred dispersion relation for the RT instability when density gradients and/or viscosity or surface tension are present.

We end this section by discussing briefly the properties of Eq. (7). Introducing the cutoff wave number k_c associated with surface tension,

$$k_c=[(\rho_2-\rho_1)g/T^{(s)}]^{1/2}\ , \tag{11}$$

Eq. (7) reads

$$\gamma^2+2k^2\nu\gamma-gkA\left[1-\frac{k^2}{k_c^2}\right]=0\ , \tag{12}$$

and the two roots are

$$\gamma_\pm=-k^2\nu\pm\left[k^4\nu^2+gkA\left[1-\frac{k^2}{k_c^2}\right]\right]^{1/2}\ . \tag{13}$$

Of course, in the inviscid tensionless limit where $\nu=T^{(s)}=0$ we recover the classical result, $\gamma_\pm=\pm\sqrt{gkA}$.

We will refer to the larger root, γ_+, simply as γ. As a function of k, $\gamma(k)=0$ at $k=0$, it increases to a peak value γ_{peak} at some $k=k_{\text{peak}}$, beyond which γ decreases and vanishes at $k=k_c$. The vanishing point, k_c, is independent of viscosity. If $k_c=\infty$ (no surface tension) then γ vanishes according to $\gamma\to gA/2k\nu$ as $k\to\infty$.

Unfortunately the value of γ_{peak} cannot be found analytically when surface tension and viscosity are *both* present: differentiating Eq. (12) with respect to k and setting $\partial\gamma/\partial k=0$ we get

$$\gamma_{\text{peak}}=\frac{gA}{4\nu k_{\text{peak}}}\left[1-\frac{3(k_{\text{peak}})^2}{k_c^2}\right]\ . \tag{14}$$

This is simple enough, but k_{peak} must be found by solving a quintic equation

$$k^3\left[\frac{k^2}{k_c^2}+1\right]-\frac{gA}{8\nu^2}\left[1-\frac{3k^2}{k_c^2}\right]^2=0\ , \tag{15}$$

obtained by substituting Eq. (14) back into Eq. (12). An alternative expression for γ_{peak} is

$$\gamma_{\text{peak}}^2=\frac{gkA}{2}\left[1+\frac{k^2}{k_c^2}\right],\quad k=k_{\text{peak}}\ , \tag{16}$$

but the main difficulty is still that of finding k_{peak}.

Let us find k_{peak} and γ_{peak} explicitly in two opposite limits: (i) surface tension dominates with viscosity being a small perturbation; and (ii) viscosity dominates with surface tension being a small perturbation (of course if there is neither surface tension nor viscosity then there is no k_{peak}). We find (i)

$$k_{\text{peak}}=\frac{k_c}{\sqrt{3}}\left[1-\left[\frac{8}{9\sqrt{3}}\right]^{1/2}R^{3/4}\right]\ , \tag{17a}$$

$$\gamma_{\text{peak}}=\left[\frac{2}{3\sqrt{3}}gk_cA\right]^{1/2}[1-(2\sqrt{3})^{-1/2}R^{3/4}]\ , \tag{17b}$$

and (ii)

$$k_{\text{peak}}=\frac{1}{2}\left[\frac{gA}{\nu^2}\right]^{1/3}\left[1-\frac{7}{12R}\right]\ , \tag{18a}$$

$$\gamma_{\text{peak}}=\frac{1}{2}\left[\frac{g^2A^2}{\nu}\right]^{1/3}\left[1-\frac{1}{6R}\right]\ . \tag{18b}$$

The dimensionless ratio R in Eqs. (17) and (18) is defined by

$$R\equiv(\rho_2+\rho_1)(gA\nu^4)^{1/3}/T^{(s)}\ , \tag{19}$$

and is a measure of the strength of viscosity vis-à-vis surface tension. The two opposite limits represented in Eqs. (17) and (18) correspond to $R\ll1$ and to $R\gg1$, respectively.

The leading terms of Eqs. (17) and (18) reproduce the behavior of γ described in the Introduction: $(\gamma^2/gkA)_{\text{peak}}=\frac{2}{3}$ (pure surface tension) or $\frac{1}{2}$ (pure viscosity). The four negative signs in front of the next-to-leading terms in Eqs. (17) and (18) imply that the locations of the peaks as well as the values of the peaks are reduced as either one of the stabilizing mechanisms, viscosity or surface tension, is added to the other.

As far as we know no experiments have been carried out to study quantitatively the effect of viscosity on the

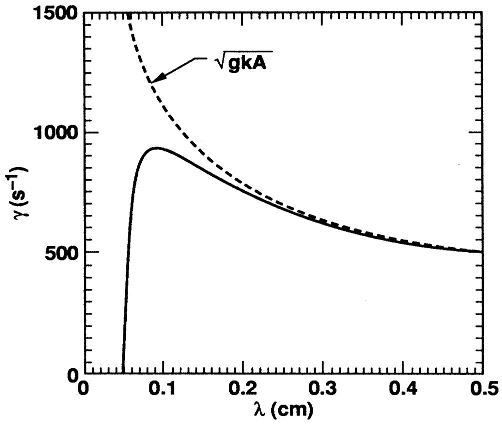

FIG. 1. The growth rate γ as a function of perturbation wavelength λ for experiment 85 of Ref. [19]. The parameters are $g=42g_0$ ($g_0=980$ cm/s^2), $\rho_1=0.66$ g/cm^3, $\mu_1=0.31$ CP, $\rho_2=1.89$ g/cm^3, $\mu_2=3.3$ CP, and $T^{(s)}=3$ dyn/cm (a surfactant was added to reduce the surface tension between the two fluids, hexane and a NaI solution). The cutoff wavelength is $\lambda_c=0.05$ cm and peak γ occurs at $\lambda_{\text{peak}}=0.09$ cm. The dashed line is $\gamma_{\text{classical}}=\sqrt{gkA}\approx 353\lambda^{-1/2}$ for γ measured in s^{-1} and λ in cm.

RT instability (the qualitative effect is obviously a common experience.) Experiments with air-water interfaces [18] are dominated by surface tension. Similarly for rocket-rig experiments to study turbulent mixing at fluid interfaces [19]. This is no surprise because the fluids were purposely chosen to reduce the effect of viscosity and surface tension (surfactants were added for the latter).

Let us illustrate with experiment 85 of Ref. [19] which had the lowest surface tension. The fluids were hexane and a NaI solution with the following properties: $\rho_1=0.66$ g/cm^3, $\mu_1=0.31$ CP (centipoise), $\rho_2=1.89$ g/cm^3, $\mu_2=3.3$ CP, $T^{(s)}=3$ dyn/cm. The acceleration was $42g_0$ ($g_0=980$ cm/s^2). From Eq. (19) we find

$$R\approx 0.08$$

and therefore surface tension still dominates. The cutoff wave number k_c is 130 cm^{-1}; i.e., wavelengths shorter than 0.05 cm are stable. From Eq. (17a) we find that the growth rate peaks at $k_{\text{peak}}=67$ cm^{-1}, with the effect of viscosity being about 10%. Such very short wavelengths ($\lambda_{\text{peak}}=0.09$ cm) quickly saturate in these experiments where mixing widths of several centimeters are observed. In Fig. 1 we plot γ vs λ and compare it with the classical growth rate $\sqrt{gkA}$.

III. RM INSTABILITY

To calculate the stabilizing effect of viscosity on the RM instability we will follow Richtmyer's approach of treating a shock as an instantaneous acceleration of incompressible fluids, i.e., let $g\to\Delta v\,\delta(t)$. In this approach the shock is viewed as an infinitely large acceleration acting for an infinitesimally short period of time such that the imparted jump velocity, $\Delta v=\int g\,dt$, is finite. We have used the same approach before in treating density gradients [20], shocks in spherical geometry [21], as well as the effect of surface tension [7].

Richtmyer treated the classical inviscid tensionless case for which $d^2\eta/dt^2=\gamma^2\eta=gkA\eta\to\Delta v\,\delta(t)kA\eta$, hence $\eta(t)=\eta(0)[1+\Delta vkAt]$. Here t is time and $\eta(t)$ is the amplitude of the perturbation at the interface between the two fluids. After the passage of a shock $g=0$ and perturbations grow linearly with time with a slope, $d\eta/dt$, set by the shock.

We present first a general formalism which can be used to find how Richtmyer's result is affected by stabilizing (or destabilizing?) mechanisms. We start with the RT case. In general, there are two exponential growth rates which we denote by $\gamma_\pm$ (they need not be given by Eq. (13), although in our specific application they will):

$$\eta(t)=a_+e^{\gamma_+t}+a_-e^{\gamma_-t}\ . \tag{20a}$$

Expressing the constants $a_\pm$ in terms of the initial conditions η_0 and $\dot\eta_0$ we get

$$\eta(t)=\eta_0\frac{\gamma_+e^{\gamma_-t}-\gamma_-e^{\gamma_+t}}{\gamma_+-\gamma_-}+\dot\eta_0\frac{e^{\gamma_+t}-e^{\gamma_-t}}{\gamma_+-\gamma_-}\ . \tag{20b}$$

This equation describes $\eta(t)$ for a constant acceleration g (g appears in the growth rates $\gamma_\pm$). The postshock evolution is also given by Eq. (20) with $g=0$ now, assuming that the shocked system is coasting and there are no postshock accelerating or decelerating external forces. In this approach the classical case appears as a singular case with $\gamma_\pm=\pm\sqrt{gkA}\to 0$.

Assuming that $\dot\eta(0_-)$, the preshock value of $\dot\eta$, is zero or very small compared to that imparted by the shock, we find that $\dot\eta_0$ in Eq. (20b) is given by $\Delta vkA\eta_0$, so that

$$\eta(t)/\eta_0=\frac{\gamma_+e^{\gamma_-t}-\gamma_-e^{\gamma_+t}}{\gamma_+-\gamma_-}+\Delta vkA\frac{e^{\gamma_+t}-e^{\gamma_-t}}{\gamma_+-\gamma_-}\ ,\quad g=0\ . \tag{21}$$

The reason for $\dot\eta_0=\Delta vkA\eta_0$ is that in the limit $g\to\infty$ we get $\gamma_\pm^2\to gkA$ at a sharp interface so that Richtmyer's evaluation of $\dot\eta_0$ is still valid.

If the interface is diffuse, (i.e., has a continuous density gradient characterized by some finite length β^{-1} (see, for example, Ref. [13]), then density gradient stabilization *survives* the limit $g\to\infty$ so that

$$\gamma_\pm^2\to\frac{gkA}{1+Ak\beta^{-1}}$$

and ΔvkA in Eq. (21) must be replaced by $\Delta vkA/(1+Ak\beta^{-1})$. Density gradient stabilization of the RM instability is discussed in more detail in Ref. [22].

Setting $g=0$ in Eq. (13) we find

$$\gamma_\pm=-k^2\nu\pm i\omega\ , \tag{22}$$

where

$$\omega\equiv\left[\frac{k^3T^{(s)}}{\rho_2+\rho_1}-k^4\nu^2\right]^{1/2}\ . \tag{23}$$

Substituting Eq. (22) into Eq. (21) we get

$$\eta(t)/\eta_0 = e^{-k^2 \nu t}\left[\cos\omega t + (k^2\nu + \Delta v k A)\frac{\sin\omega t}{\omega}\right] . \quad (24)$$

This is the generalization of Richtmyer's result to include both surface tension and viscosity.

For pure surface tension we have $\nu=0$, $\omega^2 = k^3 T^{(s)}/(\rho_2+\rho_1)$, and Eq. (24) reduces to

$$\eta(t)/\eta_0 = \cos\omega t + \Delta v k A \frac{\sin\omega t}{\omega} , \quad (25)$$

which agrees with our earlier result [7].

For pure viscosity ($T^{(s)}=0$) we get

$$\eta(t)/\eta_0 = 1 + \frac{\Delta v A}{2k\nu}(1 - e^{-2k^2\nu t}) . \quad (26)$$

Finally, if both $T^{(s)}=0$ and $\nu=0$ then we recover the classical result

$$\eta(t)/\eta_0 = 1 + \Delta v k A t . \quad (27)$$

In the case of pure viscosity Eq. (26) indicates that $\eta(t)$ increases or decreases (depending on the sign of $\Delta v A$) until it reaches the asymptotic limit of $\eta_0(1+\Delta v A/2k\nu)$. It is interesting that if the shock satisfies $\Delta v A = -2k\nu$ then this asymptote is zero—i.e., the shock completely flattens out perturbations of wavelength $4\pi\nu/|\Delta v A|$. Wavelengths twice as long, $8\pi\nu/|\Delta v A|$, undergo complete phase reversal, i.e., $\eta(t)$ goes to $-\eta_0$ asymptotically. Longer-wavelength perturbations overshoot this value before coming to rest.

The combined effect of viscosity and surface tension, Eq. (24), can be qualitatively described as follows: the oscillations come from surface tension; the damping comes from viscosity. When both are present the general motion is that of damped oscillations. Short-wavelength perturbations oscillate faster but are more damped; longer-wavelength perturbations oscillate slower and are less damped.

As in the case of pure surface tension we will illustrate Eq. (24) with two figures. Using the same parameters as in Ref. [7] we let $k_0 = 2\pi/\lambda_0$ represents a wave number corresponding to the longest wavelength λ_0, and consider wave numbers in the range $k_0 \le k \le 10k_0$. Similarly, we set the time scale by $\Delta v t_{\max} = \lambda_0$, let $A=1$, and $\omega_0 t_{\max} = 1$, where ω_0 is given by Eq. (23) with $k = k_0$. We need one more parameter here to specify the strength of viscosity relative to surface tension [we cannot use R, Eq. (19), because it involves g]. The natural parameter, we believe, is defined be setting $\omega=0$; i.e., define k^* by

$$k^* = \frac{T^{(s)}}{(\rho_2+\rho_1)\nu^2} , \quad (28)$$

so that

$$\omega = k^2\nu\left[\frac{k^*}{k} - 1\right]^{1/2} . \quad (29)$$

For $k < k^*$ ω is real and the perturbations exhibit damped oscillations. For $k > k^*$ ω is imaginary and there are no oscillations. We chose our last parameter by setting $k^*/k_0 = 50$, so that the perturbations with k in the range $k_0 \le k \le 10k_0$ have real ω's.

In Fig. 2 we show how an initially flat spectrum [which means $\eta(t=0,k)=\eta_0$ for all k] changes with time under the combined effect of viscosity and surface tension. The spectra are shown at $t=0$, $1/4t_{\max}$, $1/2t_{\max}$, $3/4t_{\max}$, and $t_{\max}$. At $t=t_{\max}$ (there is no need to stop at this time, but we did so to compare directly with the results of ref. [7]) the longest wavelength having $k=k_0$ has (almost) reached its maximum, approximately a fivefold growth, while the shorter wavelengths with $k \approx (5-10)k_0$ have already damped out. In other words, as time goes by the spectrum shifts towards longer and longer wavelengths because these are less and less damped by viscosity, although the initial "kick" of the shock, $\Delta v k A$, tends to shorter wavelength, i.e., large k's.

The evolution of individual components with $k=k_0$, $5k_0$, and $10k_0$ as a function of time is shown in Fig. 3,

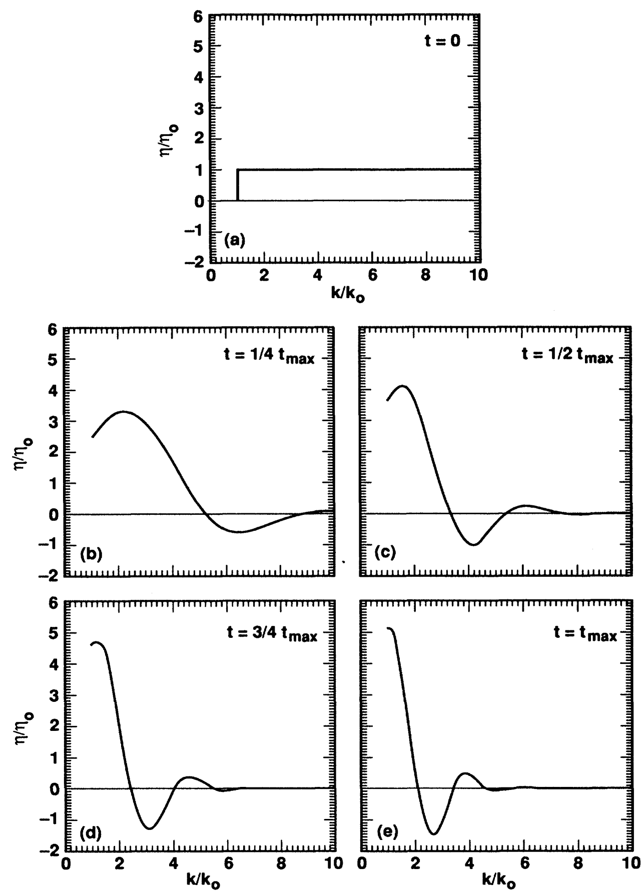

FIG. 2. Snapshots of the spectrum for a multiwavelength perturbation which is initially flat, i.e., $\eta(k)=\eta(0)$ for all k at $t=0$, immediately before a shock. We consider wave numbers in the range given by $1 \le k/k_0 \le 10$, where k_0 serves as a scale. The postshock snapshots at $t=1/4t_{\max}$, $1/2t_{\max}$, $3/4t_{\max}$, and $t_{\max}$ are calculated using Eq. (24) with the following parameters: $A=1$, $\Delta v t_{\max} = \lambda_0 = 2\pi/k_0$, $\omega_0 t_{\max} = 1$, and $k^*/k_0 = 50$. The spectrum shifts towards longer wavelengths, i.e., smaller k, because viscosity damps the shorter wavelengths. See Fig. 3 for the time evolution of representative components.

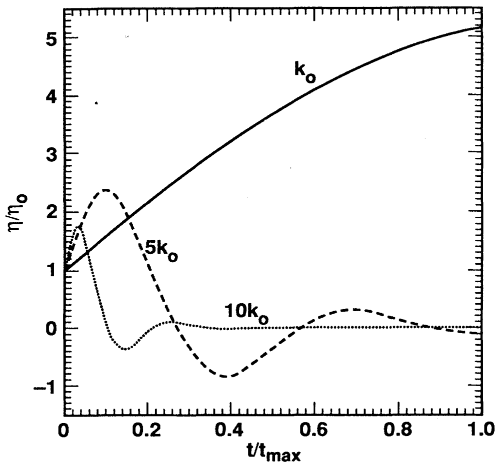

FIG. 3. The time evolution of η/η_0 for $k/k_0=1$, 5, and 10. The conditions are the same as in Fig. 2. Longer- (shorter-) wavelength perturbations oscillate slower (faster), achieve larger (smaller) maxima, and are less (more) damped by viscosity.

confirming the qualitative description given above: shorter (longer) wavelengths oscillate faster (slower), but are damped more (less). We see in Fig. 3 that at very early times the shorter wavelengths are indeed more magnified than the longer wavelengths.

This phenomenon, viz., viscosity damping perturbations at a shocked interface, must not be confused with the effect of viscosity on a rippled shock [23]. The latter is a well-known phenomenon occurring in rippled shocks passing through a *uniform* fluid and in fact the damping of the oscillations on the shock front is used to *measure* the viscosity of the fluid [23,24]. A fully compressible treatment of the RM instability in viscous fluids would have to take into account the effect of viscosity on the shock itself as well as on the motion of the interface perturbations. Our incompressible approach describes only the latter.

IV. CONCLUDING REMARKS

In this paper we generalized the $m=0$ moment equation to include the effects of surface tension and viscosity, and compared it with the $m=1$ equation corresponding to Chandrasekhar's variational principle. As in our earlier work we find that the $m=0$ equation, Eq. (4), when used with $W_{\text{classical}}$ as an approximate eigenfunction, yields better results than the $m=1$ equation, Eq. (5). It is interesting that the latter equation underestimates the growth rate γ in the presence of viscosity just as it did in the presence of density gradients, where we first made a comparison among the various moment equations [12].

We hope to have clarified Hide's derivation of Eq. (3) and Reid's comment on it: the $m=1$ equation indeed has an extra term which cannot be neglected [Hide's derivation was somewhat different: he applied Eq. (5) first to finite-thickness fluids then took the limit of semi-infinite fluids.] Hide's suggestion of using inviscid W's as an approximation is entirely reasonable and we also adopt it, except that we recommend using it in the $m=0$ equation rather than the $m=1$ equation.

In the absence of viscosity Eqs. (4) and (5) and indeed all of the higher moment equations give identical results for the classical profile (two semi-infinite inviscid fluids) because in this case $W_{\text{classical}}$ *is* the exact eigenfunction, even in the presence of surface tension. For other density or viscosity profiles we would suggest using Eq. (4) with $W=e^{-k|y-y^*|}$. Here y^* denotes the location of peak W and must be chosen judiciously [12,13].

Turning to the RM instability Figs. 2 and 3 illustrate the combined effect of surface tension and viscosity on the evolution of perturbations, as given by Eq. (24). The simple result for pure viscosity, Eq. (26), suggest that one may use this equation to *measure* viscosity. This may be more attractive than the standard way [23,24] because measuring an interface perturbation is perhaps easier than following the ripples on a shock front. Only the combination $\nu=(\mu_2+\mu_1)/(\rho_2+\rho_1)$ is available in such experiments where the measured quantity is $\eta(t)$, the time-dependent perturbation amplitude at the interface between the two fluids. From Eq. (26) the viscous exponential damping time is

$$t_\nu=1/2k^2\nu \tag{30}$$

and the asymptotic value of η is

$$\eta(\infty)/\eta(0)=1+\frac{\Delta v A}{2k\nu} \,. \tag{31}$$

As an example consider $\nu=0.1$ cm^2/s, which is typical of some oils or glycerine (ν depends on temperature), and take $\lambda=0.1$ cm. Then the exponential damping time is $t_\nu \approx 1.3$ ms. If in addition $\Delta v A=-100$ cm/s, a rather weak shock, then the asymptote is found to be $\eta(\infty)/\eta(0)=-7$, i.e., such perturbations come to rest with a final amplitude seven times larger than the initial amplitude and, of course, in opposite phase. Clearly, less viscous fluids would have much longer damping times and much larger final amplitudes, quite possibly entering the nonlinear regime, i.e., $\eta k \gg 1$. This is beyond our calculational capabilities and Eq. (26) is no longer valid.

To assess the effect of compressibility which is neglected in our analytic work we carried out two-dimensional simulations of shock tubes, with and without viscosity, on Livermore's hydrocode LASNEX. Figure 4 shows an example of our calculations: a Mach 1.3 shock passes from air into a helium test section 10 cm wide and 56 cm long, dimensions similar to the CalTech shock tube [25]. The transmitted shock, after travelling the 56 cm of He, reflects off the bottom of the shock tube and reshocks the air-He interface about 1 ms after the first shock. Figure 4 shows 10×10 cm^2 snapshots of the LASNEX mesh (which extends much farther) at $t=0.0$, 0.6, 1.0, and 1.4 ms, with the first shock arriving at $t\approx0.2$ ms. The absolute value of the perturbation amplitude $|\eta(t)|$ is plotted in Fig. 5 as a function of time with viscosity (lower curve) and without viscosity (upper curve). To highlight the effect of viscosity an artificially large value of ν, 2.2 cm^2/ms, was used in the viscous case, some four orders of

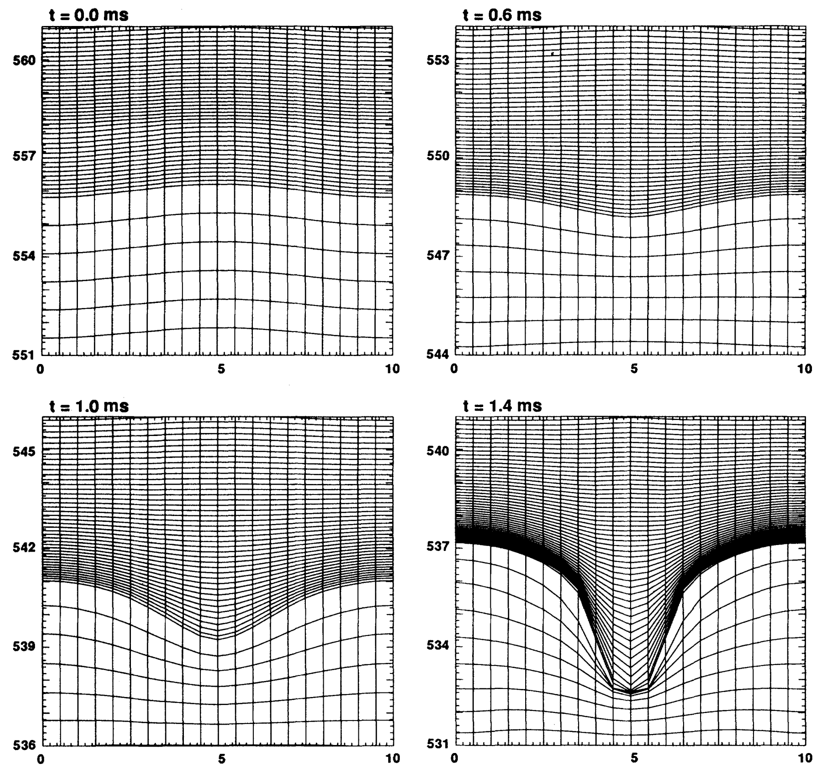

FIG. 4. Snapshots of a two-dimensional LASNEX simulation of a shock tube problem with an initial perturbation $\eta(0)=0.2$ cm at the interface between air and helium gases. The dimensions are in centimeters, with $10\times10\,\mathrm{cm}^2$ frames taken at $t=0.0$, 0.6, 1.0, and 1.4 ms. The incident and reflected shocks hit the interface at $t\approx0.2$ and 1.1 ms, respectively. There is no viscosity in this run. The perturbation amplitude $\eta(t)$ with and without viscosity is plotted in Fig. 5.

magnitude larger than the physical viscosities of air and helium.

Figure 4 shows the expected phase reversal of the perturbation since $\rho_{\mathrm{air}}\approx1.22$ mg/cm^3, $\rho_{\mathrm{He}}\approx0.17$ mg/cm^3, and therefore $A\approx-\frac{3}{4}$. We find that $\Delta v\approx20$ cm/ms so that the incompressible inviscid growth rate $\dot{\eta}=\eta_0\Delta v k A$ is about 1.9 cm/ms, a value larger than the numerical growth rate of 1.3 cm/ms seen in Fig. 5 between $t=0.5$ and 1.1 ms. This is consistent with Richtmyer's finding, viz., the effect of compressibility is to reduce the growth rate below its incompressible value. Similarly for the viscous case: the asymptotic value $\eta(\infty)$ from Eq. (31) is about -0.8 cm, i.e., $-4\eta(0)$. The compressible simulation suggests a smaller value: in Fig. 5 $\eta(t)\approx-0.3$ cm by $t\approx1.1$ ms.

The large growth in $\eta(t)$ seen in Fig. 5 after $t\approx1.1$ ms is of course induced by the above-mentioned reflected shock which, travelling now from He into air, passes through a positive Atwood number and causes growth but no phase reversal, as seen in the last snapshot of Fig. 4.

Despite the large viscosities used in the viscous case ($\mu_{\mathrm{air}}=\mu_{\mathrm{He}}=1.5\,\mathrm{mg\,cm^{-1}\,ms^{-1}}$) Fig. 5 shows that *the shock arrival times are the same with or without viscosity.* Clearly, then, viscosity cannot be measured by the one-dimensional, i.e., average motion of the shocked gases since neither shock speed nor interface velocity is affected by it, which explains why the *timing* seen in Fig. 5 is the same with or without viscosity: the incident shock arrives at $t\approx0.2$ ms and the reflected shock arrives at $t\approx1.1$ ms in both cases. However, though one cannot tell them apart based on timing, one can clearly distinguish between viscous and inviscid fluids based on the evolution of the interface perturbation $\eta(t)$.

Our final remark concerns the turbulent energy in viscous fluids undergoing a constant acceleration. We expect that certain aspects of the inviscid experiments [19,26] will continue to be valid, at least qualitatively. For example, starting with random initial perturbations a dominant scale $\lambda_0=2\pi/k_0$ will develop in the mixing layer and, as in the inviscid case, will continue to grow with time. In all likelihood the transition from the linear to the fully turbulent regime will take somewhat longer in viscous fluids. However, as the mixing width and the dominant scales continue to grow the effect of viscosity will decrease so that in the fully turbulent regime the mixing width h, which is controlled primarily by λ_0, may not deviate too much from the inviscid case. The small scales, on the other hand, will continue to sense the effect of viscosity and since $E_{\mathrm{turbulent}}$ is an integral over all scales one naturally expects it to remain below its inviscid limit.

There are no experimental results on λ_0 or $E_{\mathrm{turbulent}}$ even for inviscid tensionless fluids. The rocket-rig experiments [19,26] report h, the mixing width into the heavier fluid, as given by

$$h=0.07\,Agt^2\ . \tag{32}$$

Considering the potential energy lost by a "falling" fluid we estimated [27]

$$E_{\text{turbulent}} = Agh/6 = (\tfrac{0.07}{6}) A^2 g^2 t^2 \ . \tag{33}$$

An alternative approach is to apply the turbulence model of Ref. [28] which involves the growth rate γ. Using $\gamma = \sqrt{gkA}$ we derived [27]

$$E_{\text{turbulent}} = \frac{1}{3\pi} \left[\frac{56}{9\pi} \right]^2 Ag\lambda_0 \tag{34}$$

which agrees with Eq. (33) if

$$\lambda_0 = \frac{\pi}{2} \left[\frac{9\pi}{56} \right]^2 h \approx 0.40h \ . \tag{35}$$

The advantage of this approach is that one can link directly the reduction in γ to a reduction in $E_{\text{turbulent}}$, as we did earlier for surface tension [7] and for ablative stabilization [29]. Just as adding viscosity to surface tension further reduces the growth rate γ, we find that adding viscosity causes further reduction in $E_{\text{turbulent}}$, which can be understood as viscous heat draining away some of the potential energy and thereby making less energy available to appear as turbulent kinetic motion in the mixing layer. Therefore Eqs. (33) and (34) must be viewed as upper bounds.

Plans to measure $E_{\text{turbulent}}$ in the Boussinesq limit, $\rho_1 \sim \rho_2$, are in progress [30]. Although the scaling with g cannot be tested (g_0, the Earth's gravitational acceleration, is used in these experiments), the scaling $E_{\text{turbulent}} \sim A^2 t^2$ and $\lambda_0 \sim h$ may soon be tested experimentally.

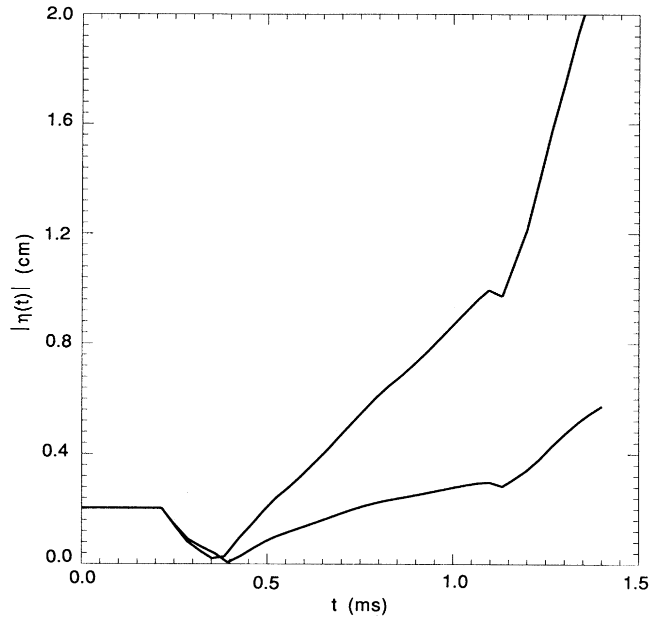

FIG. 5. $|\eta(t)|$ vs t for the shock tube problem discussed in the text. The upper curve is the inviscid case, $\mu_1 = \mu_2 = 0$; the lower curve is the same problem with $\mu_1 = \mu_2 = 1.5$ mg cm^{-1} ms^{-1}.

ACKNOWLEDGMENT

This work was performed under the auspices of the U.S. Department of Energy by the Lawrence Livermore National Laboratory under Contract No. W-7405-ENG-48.

[1] Lord Rayleigh, *Scientific Papers* (Dover, New York, 1965), Vol. 2.
[2] G. I. Taylor, Proc. R. Soc. London, Ser. A **201**, 192 (1950).
[3] R. Bellman and R. H. Pennington, Q. Appl. Math. **12**, 151 (1954).
[4] S. Chandrasekhar, *Hydrodynamic and Hydromagnetic Stability* (Oxford University Press, London, 1968); Proc. Cambridge Philos. Soc. **51**, 162 (1955).
[5] R. D. Richtmyer, Commun. Pure Appl. Math. **13**, 297 (1960).
[6] E. E. Meshkov, Izv. Akad. Nauk SSSR, Mekh. Zhidk. Gaza **5**, 151 (1969).
[7] K. O. Mikaelian, Phys. Rev. A **42**, 7211 (1990).
[8] For a review, see D. H. Sharp, Physica D **12**, 3 (1984); H. J. Kull, Phys. Rep. **206**, 197 (1991).
[9] P. Mulser, Laser Part. Beams **6**, 119 (1988). Recent calculations suggest, however, that the effect of viscosity in plasmas is much larger than calculated using classical transport coefficients—see M. Casanova, O. Larroche, and J. -P. Matte, Phys. Rev. Lett. **67**, 2143 (1991).
[10] J. Nuckolls, L. Wood, A. Thiessen, and G. Zimmerman, Nature (London), **239**, 139 (1972); S. E. Bodner, Phys. Rev. Lett **33**, 761 (1974). For a recent review see Kull, Ref. [8].
[11] D. L. Youngs, Physica D **12**, 32 (1984); Phys. Fluids A **3**, 1312 (1991). Simulations with physical viscosity were reported by G. Tryggvason and S. O. Unverdi, Phys. Fluids A **2**, 656 (1990).
[12] K. O. Mikaelian, Phys. Rev. A **33**, 1216 (1986).
[13] K. O. Mikaelian, Phys. Rev. A **40**, 4801 (1989).
[14] R. Hide, Proc. Cambridge Philos. Soc. **51**, 179 (1955).
[15] W. H. Reid, Proc. Cambridge Philos. Soc. **57**, 415 (1961).
[16] R. Menikoff, R. C. Mjolsness, D. H. Sharp, and C. Zemach, Phys. Fluids **20**, 2000 (1977).
[17] This is Eq. (88) of Chap. X in S. Chandrasekhar's book (see Ref. [4]).
[18] J. W. Jacobs and I. Catton, J. Fluid Mech. **187**, 353 (1988).
[19] K. D. Burrows, V. S. Smeeton, and D. L. Youngs, Atomic Weapons Establishment Report No. O22/84, 1984 (unpublished).
[20] K. O. Mikaelian, Phys. Rev. A **31**, 410 (1985).
[21] K. O. Mikaelian, Phys. Rev. A **42**, 3400 (1990).
[22] K. O. Mikaelian, Phys. Fluids A **3**, 2638 (1991).
[23] A. D. Sakharov, R. M. Zaidel', V. N. Mineev, and A. G. Oleinik, Dokl. Akad. Nauk SSSR **159**, 1019 (1964) [Sov. Phys. Dok. **9**, 1091 (1965)].
[24] V. N. Mineev and R. M. Zaidel', Zh. Eksp. Teor. Fiz. **54**, 1633 (1968) [Sov. Phys. JETP **27**, 874 (1968)]. For a recent review, see G. H. Miller and T. J. Ahrens, Rev. Mod. Phys. **63**, 919 (1991).
[25] M. Brouillette and B. Sturtevant, Physica D **37**, 248 (1989); M. Brouillette, Ph.D. thesis, California Institute of

Technology, 1989.
[26] K. I. Read and D. L. Youngs, Atomic Weapons Establishment Report No. O11/83 (1983) (unpublished); K. I. Read, Physica D **12**, 45 (1984).
[27] K. O. Mikaelian, Physica D **36**, 343 (1989).
[28] V. M. Canuto and I. Goldman, Phys. Rev. Lett. **54**, 430 (1985).
[29] K. O. Mikaelian, J. Appl. Phys. **65**, 964 (1989).
[30] P. Linden (unpublished).